

Entropy Explains Metal-Insulator Transition of the Si(111)-In Nanowire Array

S. Wippermann and W. G. Schmidt

Lehrstuhl für Theoretische Physik, Universität Paderborn, 33095 Paderborn, Germany

(Received 27 May 2010; revised manuscript received 28 July 2010; published 17 September 2010)

Density functional theory calculations are performed to determine the mechanism and origin of the intensively debated (4×1) – (8×2) phase transition of the Si(111)-In nanowire array. The calculations (i) show the existence of soft phonon modes that transform the nanowire structure between the metallic In zigzag chains of the room-temperature phase and the insulating In hexagons formed at low temperature and (ii) demonstrate that the subtle balance between the energy lowering due to the hexagon formation and the larger vibrational entropy of the zigzag chains causes the phase transition.

DOI: 10.1103/PhysRevLett.105.126102

PACS numbers: 68.43.Bc, 68.35.Rh, 73.20.At, 73.63.–b

Quasi-one-dimensional (1D) electronic systems are presently attracting considerable interest, fueled on the one hand by the search for fascinating collective phenomena such as spin-charge separation. On the other hand, modulation and controlled tuning of the electrical characteristics of nanoscale structures are essential for future use in nanoelectronics. The ordered array of In nanowires that self-assembles at the Si(111) surface is one of the most fascinating and most intensively studied model systems in this context. It provides a robust test bed for studying electron transport at the atomic scale [1–3]. In addition, the experimentally observed, reversible phase transition from the metallic Si(111)- (4×1) -In structure [Fig. 1(a)] formed at room temperature (RT) to an insulating (8×2) reconstruction below 120 K [4] has provoked many fundamental questions and intensive research. The atomic structure of the low-temperature (LT) (8×2) phase as well as the driving force for the phase transition remained elusive for a long time. Only recently, density functional theory (DFT) calculations by Gonzalez *et al.* [5] led to a structural model for the (8×2) phase that explains most of the spectroscopic features assigned to the LT phase. In particular, the proposed hexagon structure [Fig. 1(b)] gives rise to a small band gap in agreement with the majority of the experimental studies, e.g., Refs. [3,6–9].

What remained an open question, however, was the nature and driving force of the metal-insulator transition. Originally, it was explained as a charge-density wave formation due to the Peierls instability [4]. However, the phase transition cannot be based on a simple charge-density wave model because only one of the metallic bands nests properly [3,6,8,10,11]. A triple-band Peierls instability has been proposed, where an interband charge transfer modifies the Fermi surface to improve nesting [8,12,13], while a periodic lattice distortion that lowers the energy has also been suggested [14–18]. On the other hand, many-body interactions were made responsible for the low-temperature phase [19]. Several theoretical studies proposed the phase transition to be of order-disorder type [5,15,20] and explained the RT phase in terms of dynamic

fluctuations between degenerate ground state structures. However, photoemission [7,21] and Raman spectroscopy [22] results have cast doubt on this model.

In the present Letter we explain the (4×1) – (8×2) phase transition on the basis of DFT calculations. In contrast to earlier work, the vibrational and electronic entropy of the In nanowire array is included in the calculations. The former is found to be sufficiently large to shift the subtle balance in the free energy between the two phases and to cause a temperature-induced metal-insulator transition.

In detail, we perform DFT calculations within the local density approximation [23] as implemented in the Vienna *ab-initio* Simulation Package (VASP) [24]. We follow Stekolnikov *et al.* [2] concerning the numerical details. The Brillouin zone (BZ) integrations in the electronic structure calculations are performed using uniform meshes equivalent to 64 points for the (4×1) unit cell. This number was increased to 3200 points for the electronic entropy calculations. Frozen-phonon calculations have been performed using a (8×4) translational symmetry that yields the Γ - and X -point modes of the (8×2) unit cell.

For a fixed stoichiometry, the ground state of the surface-supported nanowires is characterized by the

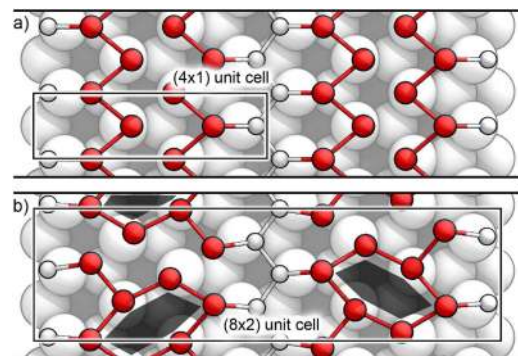


FIG. 1 (color online). Schematic top views of (a) room-temperature (4×1) and (b) the low-temperature (8×2) hexagon structure of the Si(111)-In nanowire array. Red (dark gray) balls indicate In atoms.

minimum of the free energy F as a function of the substrate crystal volume V and the temperature T . It can be obtained using atomistic thermodynamics, see, e.g., Ref. [25]. Within the adiabatic approximation, F is given by

$$F(V, T) = F_{\text{el}}(V, T) + F_{\text{vib}}(V, T), \quad (1)$$

with $F_{\text{el}} = E_{\text{tot}} - TS_{\text{el}}$, where we approximate the total energy E_{tot} by the zero-temperature DFT value and calculate the electronic entropy S_{el} from

$$S_{\text{el}} = k_B \int dE n_F [f \ln f + (1 - f) \ln(1 - f)]. \quad (2)$$

Here n_F and f denote the density of electronic states and the Fermi distribution function, respectively. The vibrational free energy of the supercell with volume Ω is calculated in harmonic approximation

$$F_{\text{vib}} = \frac{\Omega}{8\pi^3} \int d^3\mathbf{k} \sum_i \left(\frac{1}{2} \hbar \omega_i(\mathbf{k}) + k_B T \ln[1 - e^{-(\hbar \omega_i(\mathbf{k})/k_B T)}] \right). \quad (3)$$

The wave-vector dependent phonon frequencies $\omega_i(\mathbf{k})$, as well as the corresponding eigenvectors are obtained from the force constant matrix calculated by assuming $F_{\text{el}}(V, T) \sim E_{\text{tot}}(T = 0)$, i.e., neglecting the explicit temperature and volume dependence. Given the extremely flat potential-energy surface of the Si(111)-In system, that renders already the search for the minimum energy structure a difficult problem [2,15,26], we expect the uncertainty induced by the above approximations to be small compared to the overall error bar of the calculations.

The calculated Γ -point frequencies for strongly surface-localized vibrational modes of the Si(111)-In nanowire array are compiled in Table I. The table contains the present results for the (4×1) phase as well as their assignment to the frequencies of geometrically similar eigenvectors of the (8×2) phase in comparison with the Raman data from Fleischer *et al.* [22]. While measured and calculated frequencies of the (8×2) phase agree typically within a few cm^{-1} , the deviations between experiment and theory are frequently larger for the (4×1) modes. This indicates that anharmonicity effects neglected here affect the modes of the RT phase more noticeably than the LT data.

The overall good description of the distinct, but similar, sets of vibrational modes measured for the LT and RT phase by calculations for (8×2) and (4×1) geometries is another argument against the dynamical fluctuation model [5,15,20]. Also, if at elevated temperatures the system were frequently visiting configurations associated with (8×2) structures, significant contributions from the LT structure should be present in the RT spectra, in contrast to the actual experimental findings [22].

Interestingly, the calculations confirm the existence of a low-frequency shear mode of A'' symmetry for the Si(111)- (4×1) -In phase at 28 cm^{-1} . This mode, which was also detected by Raman spectroscopy [22], is energetically below the phase transition temperature of about

TABLE I. Calculated Γ -point frequencies for strongly surface-localized A' (upper part) and A'' phonon modes (lower part) of the Si(111)- (4×1) / (8×2) -In phases in comparison with experimental data [22]. The symmetry assignment of the (8×2) modes is only approximate, due to the reduced surface symmetry.

| Theory $\omega_0[\text{cm}^{-1}]$ | | Experiment $\omega_0[\text{cm}^{-1}]$ | |
|--|--------------------|--|--------------------------|
| (4×1) | (8×2) | (4×1) | (8×2) |
| 22 | 20 | 31 ± 1 | 21 ± 1.6 |
| | 27 | | 28 ± 1.3 |
| 44 | 47 | 36 ± 2 | 41 ± 2 |
| 51 | 53 | 52 ± 0.6 | 57 ± 0.7 |
| 62 | 58, 69 | 61 ± 1.3 | $62, 69 \pm 1.5$ |
| 65, 68 | 70, 69, 78, 82 | $2 \cdot 72 \pm 3.3$ | 83 ± 2.3 |
| 100, 104 | 97, 106, 113, 142 | 105 ± 1 | 100–130 |
| 129, 131 | 137, 142 | 118 ± 1 | 139 ± 1.2 |
| 143, 145 | 139, 145, 146, 147 | $2 \cdot 148 \pm 7$ | $139, 2 \cdot 154 \pm 2$ |
| 28 | 18, 19 | 28 ± 0.9 | $2 \cdot 23.5 \pm 0.8$ |
| shear mode | | | |
| \rightarrow antisym./sym. shear mode | | | |
| | 35 | | $3 \cdot 42 \pm 3.5$ |
| | 51 | | $2 \cdot 59 \pm 3$ |
| | 75 | | 69 ± 1.5 |
| | 82 | | 85 ± 1.7 |

$k_B T \sim 83 \text{ cm}^{-1}$ and has been suggested to correspond to the lattice deformation characteristic for the $(4 \times 1) \rightarrow (8 \times 2)$ phase transition [5,13,20]. The calculated eigenvector of this mode [Fig. 2(a)] shows the two In atom zigzag chains oscillating against each other. This deviates somewhat from earlier predictions [27], but agrees with recent *first-principles* molecular dynamics simulations [5,20]. In fact, we find that the structural transformation from the In zigzag-chain structure with (4×1) symmetry [Fig. 1(a)] to the In hexagons with (8×2) translational symmetry [Fig. 1(b)] can be perfectly described by superimposing the calculated eigenvector of the 28 cm^{-1} mode with the two degenerate low-frequency X point modes at 17 cm^{-1} [one of the symmetrically equivalent modes is shown in Fig. 2(b)]. Similarly, the combination of the corresponding shear mode of the Si(111)- (8×2) -In phase at 18 cm^{-1} with the hexagon rotary mode at 27 cm^{-1} [Fig. 2(c)] transforms the In hexagons back to parallel zigzag chains. The calculated phonon modes support the geometrical path for the phase transition proposed in Refs. [5,13,20]. In fact, they give an atomistic interpretation of the triple-band Peierls model [8,13,28]: The soft shear mode lifts one metallic band above the Fermi energy, while the rotary modes lead to a band gap opening for the remaining two metallic In surface bands.

What, however, is causing the phase transition? Before we discuss the difference in the free energies calculated for the two phases of the Si(111)-In surface (cf. Figure 3), a word of caution is in order. As pointed out above, the weak

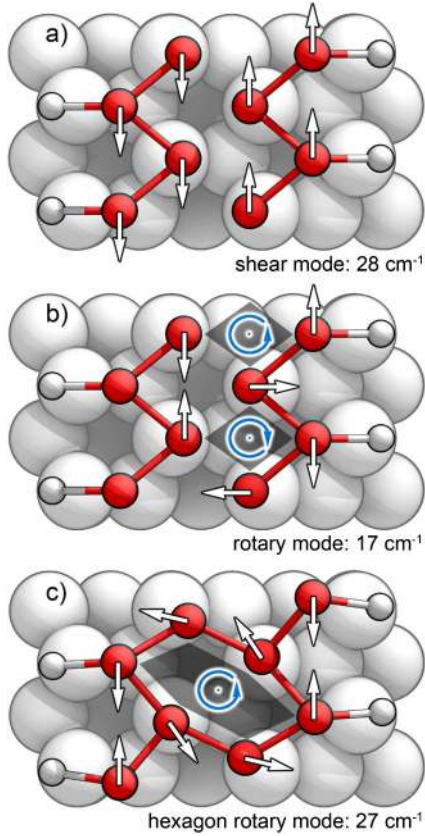


FIG. 2 (color online). Calculated eigenvectors for three prominent phonons modes (notation as in Table I) of the Si(111)-(4 × 1)-In (a),(b) and Si(111)-(8 × 2)-In phase (c). The mode shown in (b)—occurring at the X point of the (4 × 1) BZ—is twofold degenerate due to the existence of an equivalent mode at the neighboring In chain.

corrugation of the In atom potential-energy surface leading to small and error-prone force constants as well as the harmonic approximation impair the accuracy of the calculated phonon frequencies. In order to minimize systematic errors, we compare results obtained for supercells of identical size and use identical numerical parameters. The calculations are performed at the equilibrium lattice constant. From calculations where the measured lattice expansion has been taken into account, we estimate the corresponding error to be of the order of 0.1 meV per surface In atom. The sampling of the phonon dispersion curves is another crucial point. It is performed here by using only the Γ and the X point of the (8 × 2) BZ. Further restriction of the BZ sampling to the Γ point results in an energy shift of less than 0.3 meV, see inset of Fig. 3. This indicates that the unit cell is large enough to compensate for poor BZ sampling. Stekolnikov and co-workers [2] have shown that the energetics of the In nanowires depends sensitively on the functional used to model the electron exchange and correlation energy and the treatment of the In $4d$ electrons. We find the inclusion of the In $4d$ states and/or the usage of the generalized gradient rather than the

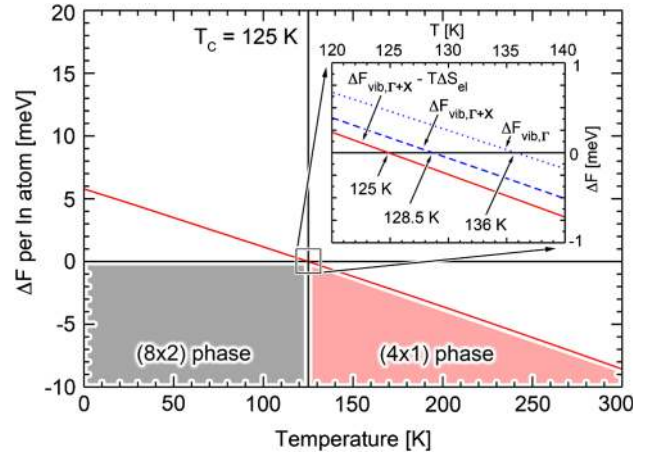


FIG. 3 (color online). Difference of the free energy $F(T)$ calculated for the (4 × 1) and (8 × 2) phase of the Si(111)-In nanowire array. The stable phase is indicated. The inset (enlarged) shows the entropy difference calculated by neglecting the electronic contributions and by restricting the BZ sampling to the Γ point.

local density approximation to result in typical (maximum) frequency shifts of $\pm 2(4)$ cm^{-1} . This affects the vibrational free energy by at most 1 meV per surface In atom at 130 K.

In Fig. 3 we present the free energy difference between the Si(111)-(4 × 1)-In and Si(111)-(8 × 2)-In phases. It vanishes at 128.5 K if only the vibrational entropy is taken into account. Additional consideration of the electronic entropy lowers the calculated phase transition temperature to 125 K. At this temperature, the vibrational and electronic entropy is large enough to compensate for the lower total energy of the insulating (8 × 2) phase compared to the metallic (4 × 1) phase. The calculated phase transition temperature is slightly above the experimental value of about 120 K. However, given the approximations and uncertainties discussed above, the agreement between theory and experiment should be considered to be fortuitously close.

The present calculations show that the phase transition is caused by the gain in (mainly vibrational) entropy that overcompensates for higher temperatures the gain in band-structure energy realized upon transforming the metallic In zigzag chains into semiconducting In hexagons. Is it possible to trace the change in vibrational entropy to the frequency shift of a few illustrative modes? Because of the reduced symmetry of the hexagon structure, the phase transformation results in modified phonon eigenvectors. This complicates the one-to-one comparison of the vibrational frequencies. However, a general trend to higher surface phonon frequencies upon hexagon formation is clearly observed. This can be seen from most values in Table I—with the shear mode as a notable exception—as well as from the comparison of the respective phonon densities of states shown in Fig. 4. The present calculations

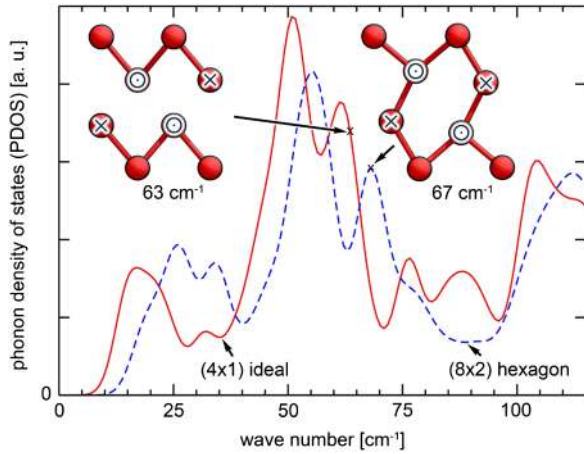


FIG. 4 (color online). Phonon density of states calculated for the (4×1) and (8×2) phases of the Si(111)-In nanowire array (4 cm^{-1} broadening). The inset shows a specific displacement pattern that hardly changes upon the phase transition but shifts in frequency. Circles/crosses indicate up/down movements.

essentially confirm earlier experimental work that states “all major modes of the (4×1) surface are found in the (8×2) spectra, though blueshifted” [22]. A typical example is shown as inset in Fig. 4. The eigenvector corresponding to the alternating up and down movements of the In atoms hardly changes upon the (4×1) – (8×2) phase transition. The according frequency, however, goes up from 63 to 67 cm^{-1} . This shift in frequency is easily understood from the formation of additional In-In bonds upon hexagon formation, resulting in larger force constants.

In summary, free energy calculations based on density functional theory are performed that explain the (4×1) – (8×2) phase transition of the Si(111)-In nanowire array in terms of a subtle interplay between the lower total energy of the insulating In hexagon structure and the larger vibrational and electronic entropy of the less tightly bound and metallic In zigzag chain structure at finite temperatures. Both the (4×1) and (8×2) phases are stable and well-defined structural phases. Soft shear and rotary vibrations transform between the In zigzag chains stable at room temperature and the hexagons formed at low temperatures. The present work resolves the discrepancies arising from the interpretation of the (4×1) reconstruction as time-averaged superposition of (8×2) structures given by the dynamic fluctuation model. It clarifies the long-standing issue of the temperature-induced metal-insulator transition in one of the most intensively investigated quasi-1D electronic systems. We expect the mechanism revealed here to apply to many more quasi-1D systems

with intriguing phase transitions, e.g., Au nanowires on high-index silicon surfaces.

We gratefully acknowledge financial support from the DFG as well as supercomputer time provided by the HLRS Stuttgart and the Paderborn PC².

-
- [1] T. Kanagawa *et al.*, *Phys. Rev. Lett.* **91**, 036805 (2003); C. Liu, T. Uchihashi, and T. Nakayama, *Phys. Rev. Lett.* **101**, 146104 (2008); Y. Terada *et al.*, *Nano Lett.* **8**, 3577 (2008); H. Shim *et al.*, *Appl. Phys. Lett.* **94**, 231901 (2009); S. Wippermann, N. Koch, and W. G. Schmidt, *Phys. Rev. Lett.* **100**, 106802 (2008).
 - [2] A. A. Stekolnikov *et al.*, *Phys. Rev. Lett.* **98**, 026105 (2007);
 - [3] T. Tanikawa, I. Matsuda, T. Kanagawa, and S. Hasegawa, *Phys. Rev. Lett.* **93**, 016801 (2004).
 - [4] H. W. Yeom *et al.*, *Phys. Rev. Lett.* **82**, 4898 (1999).
 - [5] C. Gonzalez, F. Flores, and J. Ortega, *Phys. Rev. Lett.* **96**, 136101 (2006).
 - [6] S. J. Park *et al.*, *Phys. Rev. Lett.* **93**, 106402 (2004).
 - [7] Y. J. Sun *et al.*, *Phys. Rev. B* **77**, 125115 (2008).
 - [8] J. R. Ahn *et al.*, *Phys. Rev. Lett.* **93**, 106401 (2004).
 - [9] S. Chandola *et al.*, *Phys. Rev. Lett.* **102**, 226805 (2009).
 - [10] T. Abukawa *et al.*, *Surf. Sci.* **325**, 33 (1995).
 - [11] J. Guo, G. Lee, and E. W. Plummer, *Phys. Rev. Lett.* **95**, 046102 (2005).
 - [12] J. R. Ahn *et al.*, *Phys. Rev. Lett.* **93**, 106401 (2004).
 - [13] S. Riikonen, A. Ayuela, and D. Sanchez-Portal, *Surf. Sci.* **600**, 3821 (2006).
 - [14] C. Kumpf *et al.*, *Phys. Rev. Lett.* **85**, 4916 (2000).
 - [15] J.-H. Cho, D.-H. Oh, K. S. Kim, and L. Kleinman, *Phys. Rev. B* **64**, 235302 (2001).
 - [16] J.-H. Cho, J.-Y. Lee, and L. Kleinman, *Phys. Rev. B* **71**, 081310(R) (2005).
 - [17] X. Lopez-Lozano *et al.*, *Phys. Rev. B* **73**, 035430 (2006).
 - [18] K. Sakamoto, H. Ashima, H. W. Yeom, and W. Uchida, *Phys. Rev. B* **62**, 9923 (2000).
 - [19] G. Lee, S.-Y. Yu, H. Kim, and J.-Y. Koo, *Phys. Rev. B* **70**, 121304(R) (2004).
 - [20] C. González *et al.*, *Phys. Rev. Lett.* **102**, 115501 (2009).
 - [21] H. W. Yeom, *Phys. Rev. Lett.* **97**, 189701 (2006).
 - [22] K. Fleischer *et al.*, *Phys. Rev. B* **76**, 205406 (2007).
 - [23] D. M. Ceperley and B. J. Alder, *Phys. Rev. Lett.* **45**, 566 (1980).
 - [24] G. Kresse and J. Furthmüller, *Comput. Mater. Sci.* **6**, 15 (1996).
 - [25] M. Valtiner, M. Todorova, G. Grundmeier, and J. Neugebauer, *Phys. Rev. Lett.* **103**, 065502 (2009).
 - [26] J.-H. Cho and J.-Y. Lee, *Phys. Rev. B* **76**, 033405 (2007).
 - [27] F. Bechstedt, A. Krivosheeva, J. Furthmüller, and A. A. Stekolnikov, *Phys. Rev. B* **68**, 193406 (2003).
 - [28] C. Gonzalez, J. Ortega, and F. Flores, *New J. Phys.* **7**, 100 (2005).